# The Binary–Host Connection: Astrophysics of Gravitational-Wave Binaries from Host Galaxy Properties

Susmita Adhikari[1] , Maya Fishbach[2,3] , Daniel E. Holz[2,3,4,5] , Risa H. Wechsler[1,6] , and Zhanpei Fang[1]
[1] Kavli Institute for Particle Astrophysics and Cosmology and Department of Physics, Stanford University, Stanford, CA 94305, USA; susmita@stanford.edu
[2] Department of Astronomy and Astrophysics, The University of Chicago, Chicago, IL 60637, USA
[3] Kavli Institute for Cosmological Physics, The University of Chicago, Chicago, IL 60637, USA
[4] Department of Physics, The University of Chicago, Chicago, IL 60637, USA
[5] Enrico Fermi Institute, The University of Chicago, Chicago, IL 60637, USA
[6] SLAC National Accelerator Laboratory, Menlo Park, CA 94025, USA
Received 2020 January 21; revised 2020 October 5; accepted 2020 October 6; published 2020 December 8

## Abstract

Gravitational waves from the merger of binary neutron stars (BNSs) are accompanied by electromagnetic counterparts, making it possible to identify the associated host galaxy. In this work, we explore how properties of the hosts relate to the astrophysical processes leading to the mergers. It is thought that the BNS merger rate within a galaxy at a given epoch depends primarily on the galaxy's star formation history, as well as the underlying merger time-delay distribution of the binary systems. The stellar history of a galaxy, meanwhile, depends on the cosmological evolution of the galaxy through time, and is tied to the growth of structure in the universe. We study the hosts of BNS mergers in the context of structure formation by populating the UniverseMachine simulations with gravitational wave (GW) events, based on a simple time-delay model. We find that different time-delay distributions predict different properties of the associated host galaxies, including the distributions of stellar mass, star formation rate, halo mass, and local and large-scale clustering of hosts. Moreover, BNSs merging today with short delay times occur preferentially in hosts with high star formation rates, while those with long delay times live in dense regions within massive halos that have low star formation. We show that with $\mathcal{O}(10)$ events from current GW detector networks, it is possible to make preliminary distinctions between formation channels which trace stellar mass, halo mass, or star formation rate. We also find that strategies to follow-up GW events with electromagnetic telescopes can be significantly optimized using the clustering properties of their hosts.

Unified Astronomy Thesaurus concepts: Gravitational wave sources (677); Galaxy evolution (594); Cosmological evolution (336); Compact binary stars (283)

## 1. Introduction

The first gravitational wave (GW) detection of a binary neutron star (BNS), GW170817, detected by advanced LIGO (Aasi et al. 2015) and Virgo (Acernese et al. 2015), ushered in the era of GW multi-messenger astronomy (Abbott et al. 2017b, 2017c). GW170817 was observed in a broad swath of the electromagnetic spectrum, including as a short gamma-ray burst (sGRB), an X-ray/radio afterglow, and an optical kilonova (Abbott et al. 2017a, 2017c; Alexander et al. 2017; Coulter et al. 2017; Margutti et al. 2017; Soares-Santos et al. 2017).

The formation and evolutionary history of BNS systems are not well constrained (e.g., Belczynski et al. 2018). These systems are usually characterized by a delay time between the initial formation of the binary and its eventual merger. The distribution of these delay times is expected to follow the distribution of the major axes of their orbits (Peters 1964), and in the case of massive O/B stars that collapse to form compact binary objects, a power-law distribution $dN/da \propto a^{\beta}$ is assumed (Sana et al. 2012; Kobulnicky et al. 2014). The merger time-delay distribution is therefore also expected to follow a power-law distribution, $dN/dt \propto t^{\alpha}$, with some minimum time-delay, $t_{\rm d}$. In general, BNSs are expected to have $\alpha = -1$ but if the binary goes through a common envelope phase, the power-law dependence can be steeper, and closer to $t^{-1.5}$ (Dominik et al. 2012; Belczynski et al. 2018; Safarzadeh & Berger 2019).

Within the next few years, the network of GW detectors is likely to provide a statistical sample of tens to hundreds of well-localized BNS merger events (Abbott et al. 2018). It is anticipated that a significant fraction of these BNS events will be associated with electromagnetic counterparts and corresponding host galaxies (Abbott et al. 2017d; Chen et al. 2018; Palmese et al. 2019). Statistical studies of the properties of the host galaxies will provide a new window into understanding these systems. For example, a recent study by Safarzadeh & Berger (2019) proposes to use the stellar masses of BNS host galaxies to infer the time-delay distribution of neutron star mergers. In particular, they forecast the constraints on the minimum delay time $t_{\rm d}$, and the slope $\alpha$ of the time-delay distribution that will be possible in relation to future events. They find that it will require $\mathcal{O}(1000)$ GW detections with identified host galaxies to constrain the parameter space of time-delay models. With third-generation GW detectors, such as the Einstein telescope, and Cosmic Explorer, the redshift distribution of detected events alone will provide tight constraints on the star formation rate/time-delay distributions, without additional information from the host galaxies (Safarzadeh et al. 2019; Vitale et al. 2019). In the meantime, it is instructive to explore the complete range of host galaxy properties that may potentially correlate with binary evolution. In this work, we explore how the properties of galaxies hosting BNS mergers depend on BNS merger timescales. We show how a full range of galaxy observables can be used to constrain details of BNS evolution.

In addition to stellar mass, there are other host galaxy observables containing information regarding the evolution of BNS systems through cosmic time. The rate of BNS mergers in a given galaxy is a convolution of the galaxy's entire history of star formation over its lifetime and the delay time between formation and merger. Galaxies reside in the centers of dark matter halos, and their evolutionary history is tied to the evolution of the dark matter halo in the cosmic web (for a detailed review of the galaxy–halo connection, see Wechsler & Tinker 2018). Even at a fixed stellar mass, for example, star-forming and quiescent galaxies have significantly different evolutionary histories, affected by the environments of their parent dark matter halos. Additional information regarding the star formation rate of a BNS host can therefore provide important insights into its underlying formation mechanism. Recent work by Artale et al. (2020) uses a population synthesis model for BNS mergers, coupled with a hydrodynamic galaxy simulation, to predict host galaxy properties, with a focus on stellar mass and star formation rate. Their results suggest that while the BNS merger rate correlates most strongly with a galaxy's stellar mass, it also depends on the star formation rate of the galaxy.

The mass of the parent halo can also in principle be probed by a variety of mass proxies, including X-ray measurements of the virial temperature of the gas, or the velocity dispersion of the satellites or stars associated with it. The net amount of baryonic matter available for a galaxy to form stars is directly related to the depth of potential of its parent dark matter halo, leading to a correlation between a galaxy's luminosity and its halo mass. In general, high-mass halos tend to host more luminous galaxies (e.g., Kravtsov et al. 2004; Vale & Ostriker 2004); however, it has been shown that the slope of the stellar mass–halo mass relation becomes significantly shallower at high halo masses (e.g., Behroozi et al. 2013a; Kravtsov et al. 2018; Wechsler & Tinker 2018) indicating that galaxies with the same stellar mass can exist in a range of halo masses. Considering that the quenching of star formation, together with various astrophysical feedback processes that control stellar evolution in a galaxy vary as a function of the host halo potential (Silk & Rees 1998; Croton et al. 2007; Bullock et al. 2000; Hopkins et al. 2012); this implies different evolutionary channels for galaxies with similar luminosities, but different halo masses. Therefore, in principle, the host halo mass can provide complementary information to the stellar mass of a galaxy, with regard to its growth history. Furthermore, particularly at high stellar masses, where star formation appears to be quenched, the parent halo mass and environment provide additional information, independent from the star formation rate, about the merger history of the galaxy itself.

A galaxy's environment can provide additional information about the history of the galaxy (Oemler 1974; Wechsler & Tinker 2018). For example galaxies that live in dense local environments, such as clusters or galaxy groups, tend to be less star-forming and redder, while the fraction of blue, star-forming galaxies dominate the population in the field, or in low density environments (Balogh et al. 1997; Dressler 1980; Dressler & Gunn 1983). In principle, the large-scale environment of a galaxy can also play a role in its star formation history. Since halos, within which galaxies reside, form hierarchically (Bardeen et al. 1986; Bond et al. 1991), assembling through mergers of smaller halos, the nature of halo mergers and their frequency are both dictated by the environment around the initial density peak (Gao & White 2007; Wechsler et al. 2006; Dalal et al. 2008). The halo's merger history can therefore be expected to impact the history of the galaxy residing within it (Conroy & Wechsler 2009). There are many ways to parameterize this environment: one relevant cosmological measure is the density of matter in the vicinity of a galaxy at different scales, which is often measured as an abundance or number density of galaxies in the neighborhood of a target galaxy. This is an observable which is measurable in most galaxy surveys and can, in principle, through its effect on the galaxy merger history, be used to constrain the delay time distributions of binary systems.

The galaxy in which a binary forms evolves in the time between formation and the binary's eventual merger. Correlations between properties of the host galaxy at binary formation, and the properties of the host galaxy when the binary merges, can therefore, in principle, be washed out for sufficiently long delay times (Zevin et al. 2019). However, the evolution of the galaxy can be inferred by studying the properties of host galaxies extensively, in their full cosmological context. In this paper, we study a set of observational properties containing information about the evolution of the galaxy through cosmic time. To study the distribution of galaxy properties, we use the UniverseMachine simulations (Behroozi et al. 2019). These simulations populate dark matter halos in a cold dark matter (CDM), $N$-body simulation with galaxies. The connection between galaxies and their halos is based on a semi-empirical model that parameterizes the correlation between the star formation rate of a galaxy and the properties of its parent halo, including its potential well depth, redshift, and assembly history, using an extensive set of observational constraints.

GW170817 was accompanied by an sGRB; thus, there there is evidence that (at least some) sGRBs are expected to be produced by neutron star mergers. Previous studies into the host galaxies of sGRBs (Bloom et al. 2006, 2007; Prochaska et al. 2006; Berger et al. 2007; Leibler & Berger 2010; Fong & Berger 2013) have already provided important insights into the progenitors of BNS systems. A comparison between the host galaxy of GW170817 and the host galaxies of cosmological sGRBs was performed by Fong et al. (2017). Furthermore, understanding the connection between binaries and their hosts may provide novel cosmological probes, such as inferring the cosmic star formation history of the universe (Fishbach et al. 2018; Vitale et al. 2019). Characterizing the binary–host connection may also contribute to an understanding of the systematic uncertainties involved in measuring the Hubble constant from standard sirens (Schutz 1986; Holz & Hughes 2005; Dalal et al. 2006; Abbott et al. 2017d). Similar studies have already been used to elucidate the connection between supernovae and their host galaxies (Brout et al. 2019).

Here we explore the constraints on time-delay distributions, resulting from analyzing the observable properties of the host galaxies in relation to BNS mergers. In particular, we focus on the distributions of four observables: stellar mass, specific star formation rate, halo velocity dispersion (a proxy for halo mass), and the local density around the hosts of GW events. For a range of time-delay models, we forward model the distribution of host galaxy properties, using a simulated galaxy catalog. In Section 2, we describe the simulations, and in Section 3 we describe our method and main results.

## 2. Simulated Galaxy Catalogs

Given the star formation history of a galaxy and an assumed distribution of delay times between formation and merger, we can calculate the merger rate, $\mathcal{R}$, at redshift $z_f$:

$$\mathcal{R}(z_f) = \lambda \int_0^{t(z_f)} \frac{dP}{dt}(t_f - t)\Psi_g(t)dt, \qquad (1)$$

where $\Psi_g(t)$ is the star formation rate of the galaxy at time $t$, $dP/dt$ is the delay time distribution, and $\lambda$ is an efficiency factor. We consider a power-law distribution in merger times, such that $dP/dt \propto (t - t_{\rm d})^{-\alpha}$, where $t_{\rm d}$ is the minimum delay time, below which no BNS system can merge. We use $t(z)$ to convert between redshift and time, assuming Planck cosmology (Aghanim et al. 2018).

The star formation history of a galaxy depends on the galaxy properties, such as its halo mass, stellar mass, and local environment. Therefore, the observed merger rate in the universe at a given time is the convolution of the delay time distribution and the star formation rate, where the star formation rate depends on various galaxy properties.

To emulate the distribution of galaxy properties in a cosmological context, we use the UniverseMachine simulation. UniverseMachine provides a galaxy catalog, with galaxy stellar masses and star formation histories extending from $z = 0$ to $z = 10$. We use the publicly available galaxy catalogs, created using the Bolshoi–Planck simulation (Klypin et al. 2011), which is a dissipationless CDM-only $N$-body simulation of a 250 Mpc $h^{-1}$ volume with $2048^3$ particles, in a Planck Cosmology, where $\Omega_m = 0.307$, and $h = 0.7$.

To study the hosts of BNS events at $z = 0$, we track the galaxy properties of every object in the catalog with a halo mass greater than $1.35 \times 10^{10} M_{\odot} \, h^{-1}$, corresponding to halos with more than 100 particles in the simulation. We use the merger trees from the ROCKSTAR halo finder (Behroozi et al. 2013b) to reconstruct the galaxies' star formation histories across cosmic time. We then use the main branch of the merger tree, which tracks a galaxy's most massive progenitors in time, for every galaxy in the catalog. The galaxy merger history is sampled at 164 log-spaced points, between $z = 0$ and $z = 10$.

We focus on four observable properties of the galaxies: the stellar mass of the galaxy, $M_*$, the galaxy's specific star formation rate, sSFR (SFR/$M_*$), the velocity dispersion of the parent halo, $\sigma_h$, and the ratio of the local and large-scale density, $\Delta_r$. The stellar mass and specific star formation rates are provided by the simulated galaxy catalog. We use the specific star formation rate because it traces the strength of the current burst of star formation with respect to the galaxy's underlying stellar mass, correlating strongly with the observed color and morphology of a galaxy (Guzman et al. 1997; Brinchmann et al. 2004).

Meanwhile, we use the velocity dispersion of galaxies within the parent halo as an observable proxy for the total halo mass. This velocity dispersion is computed using the velocities of galaxies within a halo's virial radius. For satellite galaxies (i.e., galaxies residing in subhalos), we use the velocity dispersion of the parent halo in which the subhalo resides. For galaxies residing in low mass halos, where there is an insufficient number of resolved subhalos, we use the mass of the halo to compute the velocity dispersion. To compute the local density around a given galaxy, we measure the number density of neighboring galaxies as a function of their 3D radius from the given galaxy. We include only neighboring galaxies with stellar masses greater than $M_* = 10^9 M_{\odot} \, h^{-1}$. We define the observable $\Delta_r$ as the ratio of density within 0.6 Mpc $h^{-1}$, as compared to the density within 5 Mpc $h^{-1}$. The smaller scale is chosen to represent a galaxy's local environment, sensitive to whether or not it exists as a part of a group or a cluster of galaxies, while the larger radius is representative of its large-scale environment or neighborhood beyond its own parent halo.

In the following sections, we study the properties of the host galaxies in relation to BNS mergers, as a function of the time-delay model. We then estimate the number of events required in order to make inferences about the evolutionary history of merging binaries.

## 3. Results

### 3.1. Weighted Distributions

The underlying population of BNS systems is drawn from the distribution of stars in the universe. Among the first questions to be posed is whether BNS host galaxies are biased tracers of the underlying population of galaxies in the universe. For example, we may ask whether BNS mergers trace stellar mass, in which case they would occur preferentially in high $M_*$ galaxies (Artale et al. 2020; Ducoin et al. 2020; Toffano et al. 2019). Alternatively, BNS mergers may trace star formation rate (Phinney 1991) or halo mass, or they may be randomly distributed in galaxies with equal probability.

We ask how large a sample of host galaxies would be required in order to distinguish these simple models, where mergers trace either the stellar mass of a galaxy, the star formation rate, or the virial mass of the parent halo in which they reside. The arguments in this section are not specific to BNS systems, and can be extrapolated to black hole binaries, or black hole–neutron star mergers, assuming that their host galaxies can be identified.

Physically, we can associate a model in which BNS mergers trace the star formation rate with a zero delay time model, where binaries merge as soon as they are born. In this scenario, the merger rate would simply trace the rate at which new stars are forming in a galaxy. At the other extreme, for very long time delays on the order of 10 Gyr, we expect low-redshift BNS mergers to trace the stellar mass, as high stellar mass galaxies reached the peak of their star formation at early redshifts. Alternatively, it has been proposed that, rather than forming from isolated stellar binaries in the galactic field (Tauris et al. 2017; Vigna-Gómez et al. 2018), a significant fraction of BNSs may form via dynamical interactions in dense globular clusters (Grindlay et al. 2006; Andrews & Mandel 2019). Recent studies indicate that globular cluster abundance is a good tracer of a galaxy's host halo mass (Hudson et al. 2014; Harris et al. 2013). In this way, a BNS merger rate that traces dark matter halo mass, rather than galaxy stellar mass, could be an indication that BNS systems are preferentially formed in globular clusters. We also note that some studies suggest that formation in globular clusters is unlikely for BNS systems, but remains a viable scenario for BBHs, as massive black holes sink more efficiently to the dense centers of globular clusters, due to mass segregation (Ye et al. 2020).

Figure 1 shows the logarithmic distributions of stellar mass and specific star formation rates of host galaxies, drawn from
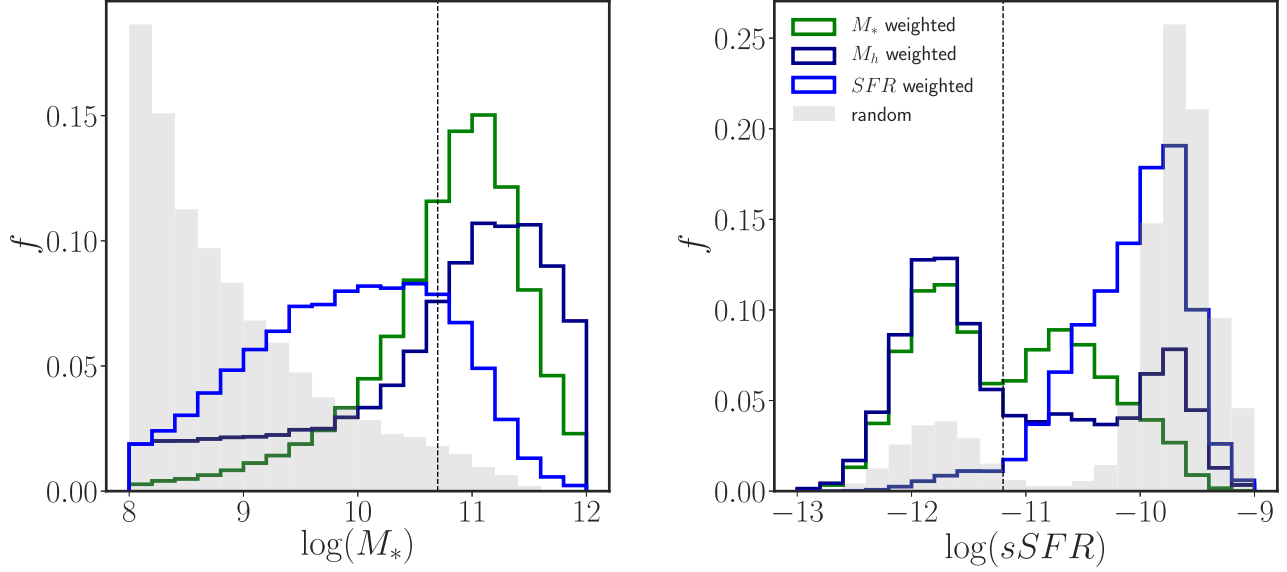
**Figure 1.** The distribution of galaxy stellar mass (left) and specific star formation rates (right) for the host galaxies, corresponding to BNS events for models where those events are weighted by different galaxy properties. We consider models in which BNS event rates are proportional to stellar mass, star formation rate, and halo mass, or in which they are randomly assigned to galaxies above our mass threshold. The vertical dotted lines denote the stellar mass and specific star formation rate of NGC 4993. We note that the distributions show significant differences, suggesting that they may be distinguished from one another with only a small number of observations of their host galaxies.

samples weighted by stellar mass, star formation rate, or halo mass. Note that all logarithmic scales used in this paper correspond to log-base 10. We have selected a minimum stellar mass threshold of $10^8 M_\odot \ h^{-1}$ for this study, and only include galaxies above this threshold. The gray shaded region corresponds to a random selection of galaxies (i.e., those with equal weights). It is evident that the distributions differ significantly from those of a random sample, as well as from each other; in principle, even a small number of events can distinguish them from one another.

To estimate the number of host galaxies required to distinguish between the $M_*$-, SFR-, and $M_h$-weighted distributions, we first construct the probability distribution of galaxies in the 4D space of observable properties, [$M_*$, sSFR, $\sigma_h$, $\Delta_r$]. We draw $10^6$ galaxies from the full galaxy catalog, with weights proportional to the various parameters. We approximate the 4D probability density as a histogram; i.e., we distribute the galaxies in bins of the observable properties and assume that the probability distribution function for model $k$, $p_k(M_*, \text{sSFR}, \sigma_h, \Delta_r)$, is piecewise constant in each bin. We use 10 bins in each direction.[7]

Given the probability distributions expected for each model, we draw 1000 samples of $N$ galaxies from each model, as well as random selections of galaxies from the galaxy catalog. We compute the likelihood of each model, $k$, given the events:

$$\mathcal{L}_k = \prod_{i=1}^{N} [p_k(M_*^i, \text{sSFR}^i, \sigma_h^i, \Delta_r^i)], \qquad (2)$$

where $p(...)$ is the piecewise constant in the bins, and where $i$ runs over each event. Finally, we compute the evidence ratio, $\mathcal{R} = \mathcal{L}_1/\mathcal{L}_2$, between them to see if the models are distinguishable.

Figure 2 shows the log evidence ratio for pure samples drawn from different models. The right panel shows comparisons between the weighted models and a random draw of galaxies. We find that we can confidently distinguish a weighted sample from a random distribution with as few as 10 events, using our complete set of observables (solid lines). The left panel shows the evidence ratio for distinguishing between the different models themselves. We find that we can distinguish a star formation rate weighted sample from a stellar mass weighted one with order of 10 events, while we begin to distinguish between a stellar mass weighted and a halo-mass weighted distribution with about 30 events. We find that even with the small samples of neutron star mergers with counterparts expected to be identified on the near future using the current generation of GW detectors, we can draw important inferences about the formation mechanisms of these systems based on the properties of their host galaxies. In fact, we expect to be able to learn about the underlying models using only the distribution of observed stellar masses, as indicated by the dashed lines in the same figure. The contribution of additional information about the remaining properties increases the weight of evidence in favor of the correct model. Although we can now begin to distinguish between the simple weighted populations, using only a few tens of events, in the next section, we investigate how well we can resolve the time-delay distribution.

### 3.2. Delay Time Distributions

As described in Section 2, the rate of BNS mergers in a given galaxy is a convolution of the delay time distribution of the BNS systems with the star formation rate of the galaxy over its history (Equation (1)). For an assumed time-delay distribution, characterized by a slope, $\alpha$, and a minimum delay time, $t_d$, we forward model the merger rate at $z = 0$ for every galaxy in our catalog, using its star formation history. These star
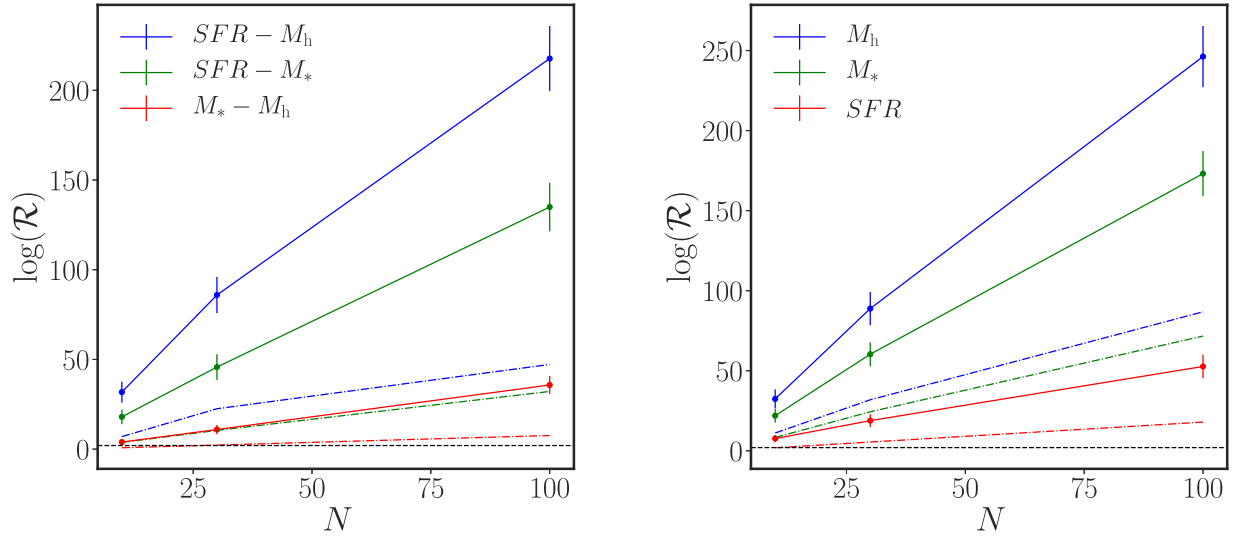
---

[7] We find that our analysis is insensitive to the number of bins. We also test our results using kernel density estimation rather than histograms, finding that our results are consistent.

**Figure 2.** (Left) The logarithmic evidence ratio as a function of the number of events between models, weighted by stellar mass and halo mass (red), stellar mass and star formation rate (blue), and halo mass and star formation rate (green). (Right) The evidence ratio between a random sample of galaxies and a weighted sample of galaxies. The dashed colored lines correspond to the evidence ratio when only the $M_*$ distribution of the host galaxies are used. The horizontal, dashed, black line corresponds to a ratio of 99.7; points above this imply that models can be distinguished with greater than $3\sigma$ confidence.

formation histories are extracted from simulated merger trees, constructed via the UniverseMachine.

Figure 3 shows the average star formation history of galaxies of different stellar masses (where stellar mass refers to $z = 0$). Today's massive galaxies tend to reach the peak of their star formation at earlier times, as compared to low mass galaxies. On the other hand, late time ($z \lesssim 0.5$) star formation histories are fairly flat, particularly in the case of low mass galaxies. Star-forming and quiescent galaxies also tend to populate different regions of the universe. In particular, galaxies in clustered environments today are on average more quiescent than galaxies inhabiting isolated environments.

To build intuition as to how different delay times influence the properties of host galaxies, we consider an illustrative example in which the delay time distribution, $dP/dt$, is a delta function, $\delta(t - t_d)$. This corresponds to the scenario where all binaries merge instantly after a delay time, $t_d$, subsequent to their formation. For a given delay time, the galaxies at $z = 0$ most likely to host a BNS merger are those that were forming the highest number of stars at the cosmological lookback time corresponding to the fixed $t_d$. Figure 4 shows the probability distribution of GW events in the space of stellar mass and specific star formation rate for galaxies at $z = 0$ for different, fixed delay times. The left panel shows the probability of a galaxy, with a given $M_*$ and sSFR today, hosting mergers over a very short delay time. The dark blue band of highest probability follows galaxies with the highest total star formation rate (a product of their stellar mass and specific star formation rate) today. As the delay time increases, i.e., from the left to right panels, we see that the blue high-probability region shifts to galaxies with high stellar masses today. The extreme right panel corresponds to $t_d \sim 10$ Gyr. For such a long delay time, BNSs merging in galaxies at $z = 0$ were formed in galaxies at $z \sim 1$, corresponding to the peak in star formation for massive galaxies. Even though these massive galaxies have low star formation rates today, they dominated the star formation in the universe at $z = 1$; as we shift from short to long time delays, the merger rate shifts from tracing SFR to stellar mass. Because the host galaxy of GW170817, NGC
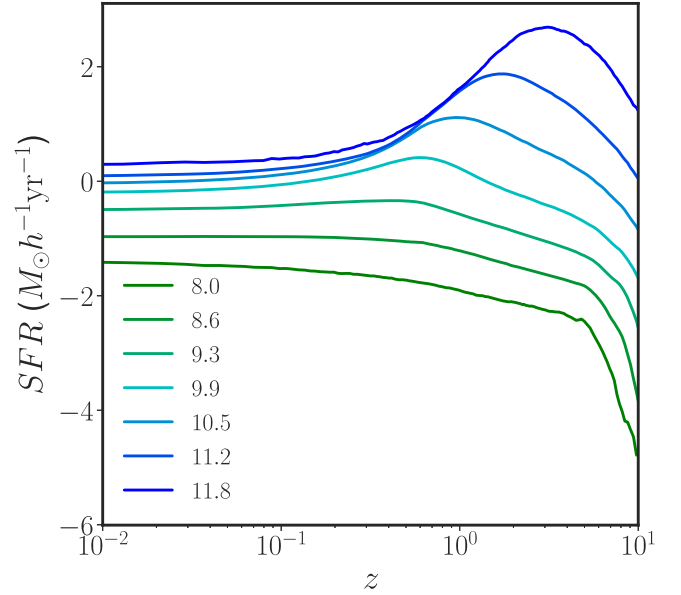


**Figure 3.** Average star formation histories for different logarithmic stellar mass bins. The colors range from green to blue, corresponding to low and high $z = 0$ stellar masses in units of $M_\odot h^{-1}$. Galaxies with high stellar mass at $z = 0$ reach the peak of their star formation at higher redshifts.

4993, has relatively high stellar mass, but not a high star formation rate, this single host galaxy exhibits a mild preference for long time delays. (Blanchard et al. 2017; Levan et al. 2017; Pan et al. 2017; Belczynski et al. 2018).

Where Figure 4 demonstrates the distribution of host galaxies in the $M_*$–sSFR plane, Figure 5 shows the distribution of velocity dispersion (a proxy for halo mass) and density ratio (a measurement of the local environment density) of the BNS hosts. We now consider a power-law distribution of delay times, rather than a $\delta$-function, varying the minimum delay time, as well as the slope of the delay time distribution. For long delay times, BNS mergers preferentially occur in more massive halos, following the correlation between stellar mass and halo mass. This means that as the delay time is increased,
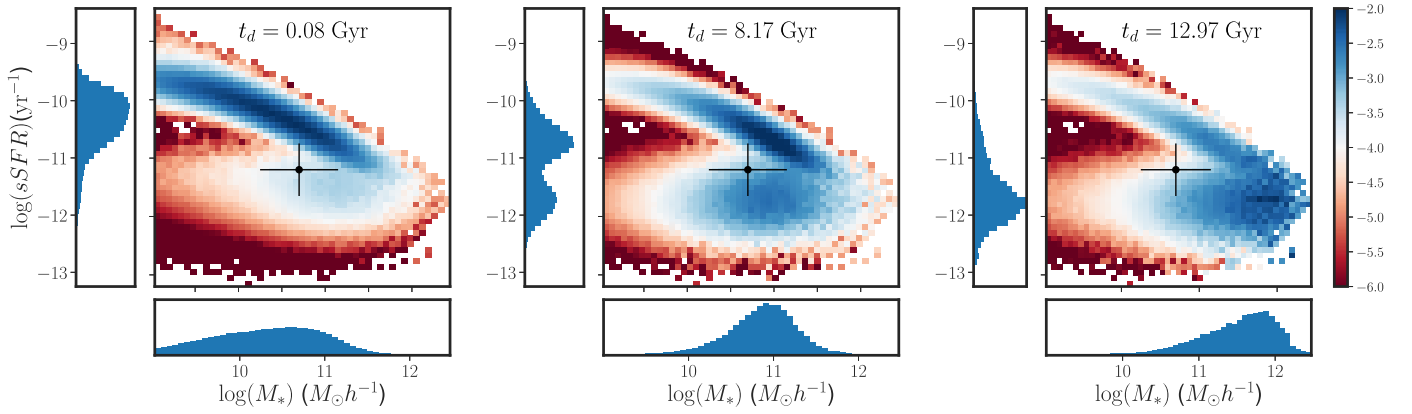
**Figure 4.** Distribution of events in the sSFR–$M_*$ plane for host galaxies at $z = 0$, for a delta function delay time distribution, with time-delay $t_{\rm d}$. The three panels, from left to right, illustrate progressively longer time delays. The cross-bar is the position of NGC 4993.

the peak of the distribution of velocity dispersions in Figure 5 moves to larger values. Here, we stress that for satellite galaxies (i.e., those inhabiting subhalos), the velocity dispersion refers to that of the parent halo in which the galaxy resides. The halo mass distribution is not particularly sensitive to the slope of the delay time distribution, if it is varied between $-1$ and $-1.5$, except for fairly short minimum delay times.

In the right panel of Figure 5, we show the distribution of the local galaxy density, $\Delta_r = \Delta_{0.6\,{\rm Mpc}h^{-1}}/\Delta_{5\,{\rm Mpc}\,h^{-1}}$ surrounding BNS host galaxies at $z = 0$. We measure the number density of galaxies with a stellar mass greater than $10^8 M_\odot\ h^{-1}$ enclosed within different spherical volumes around each host galaxy. The distribution of enclosed densities at large scales, of order $\sim 5\,{\rm Mpc}\,h^{-1}$, traces the overall bias of the halo, while the enclosed density at smaller scales, $\sim 0.5$ Mpc $h^{-1}$, traces the local environment of a halo. For galaxies residing in clusters or group-like environments, the small scale density should be higher. A high local density is correlated with high star formation rate at earlier times. As star formation histories are sensitive to the local environment, we find that the different delay time models lead to significantly different clustering properties among the host galaxies.

We now address how well we can expect to constrain the delay time distribution with a given number of BNS mergers within identified host galaxies. As in the case of the weighted models described above, for each time-delay distribution, we first construct the probability distribution of $z = 0$ host galaxies in the observable space of $M_*$, sSFR, $\sigma_h$, and $\Delta_r$. We assume power-law time-delay distributions, and consider a wide range of minimum delay times, $0.1 < t_{\rm d} < 12$ Gyr, and slopes, $-4 < \alpha < 0$. Given $N$ host galaxy observations, we can use the forward-modeled distributions of galaxy properties to calculate the likelihood that the $N$ host galaxies came from a time-delay distribution with minimum delay $t_{\rm d}$ and slope $\alpha$. We consider a case in which we only have access to the stellar masses and star formation rates of the observed host galaxies, as well as a case in which the velocity dispersions and local densities are also available.

In the coming years, we expect tens to hundreds of BNS detections; in Figure 6, we show the projected constraints from 30 and 100 events with identified host galaxies. We consider three different time-delay distributions with differing minimum delays and slopes, and show how well we can constrain each distribution. The shaded regions denote $1\sigma$ contours around each point. As a proof of concept, in this work, we assume that

the galaxy properties are perfectly measured (i.e., zero measurement uncertainty), and that each BNS merger is equally likely to have an identified host galaxy (i.e., there are no selection effects that bias host galaxy selection). This method can easily be extended to incorporate measurement uncertainty and selection effects if these prove to be significant.

We observe that using the velocity dispersion and the local density information relating to the host galaxies, along with their star formation rates and stellar masses, produces tighter constraints than those achieved using only the stellar mass information. We find that, based on $\sim 100$ events, we can constrain time delays with Gyr precision, and can confidently distinguish between low, moderate, and high minimum time delays. At small values of $t_{\rm d}$, there is significant degeneracy between $\alpha$ and $t_{\rm d}$. We also note that for large time delays (above 4 Gyr), we lose our ability to constrain the slope of the merger time distributions (the contours are vertical).

### 3.2.1. NGC 4993

We assess our findings in the context of the BNS merger GW170817 and its host galaxy NGC 4993. Currently, GW170817 is the only BNS merger to be detected in GWs. Following the GW detection, electromagnetic searches of the GW localization volume succeeded in identifying its optical counterpart, and associated host galaxy, NGC 4993 (Coulter et al. 2017; Soares-Santos et al. 2017; Abbott et al. 2017c). NGC 4993 has a stellar mass of $0.3$–$1.2 \times 10^{11} M_\odot$ and an average star formation rate over a Gyr of $10^{-0.5} M_\odot\,{\rm yr}^{-1}$ (Artale et al. 2019). Given its high stellar mass and low star formation rate, it seems likely that NGC 4993 is drawn from a population that traces stellar mass more closely than star formation rate (see Figure 1). Given this single host galaxy, we use its position on the $M_*$–sSFR plane to estimate the likelihood of different models. To account for the error bar in the measurement of $M_*$ and sSFR, we smooth the probability distributions while computing the likelihoods, such that

$$p(M_*^{\rm obs}, {\rm sSFR}^{\rm obs}|H)$$
$$\propto p(M_*^{\rm obs}, {\rm sSFR}^{\rm obs}|M_*, {\rm sSFR})p(M_*, {\rm sSFR}|H), \quad (3)$$

where $p(M_*^{\rm obs}, {\rm sSFR}^{\rm obs}|M_*, {\rm sSFR})$ is a 2D Gaussian with given mean and standard deviation that corresponds to the $M_*$ and sSFR of NGC 4993, and $H$ is a model or a model and its parameters $\alpha$, and $t_{\rm d}$.
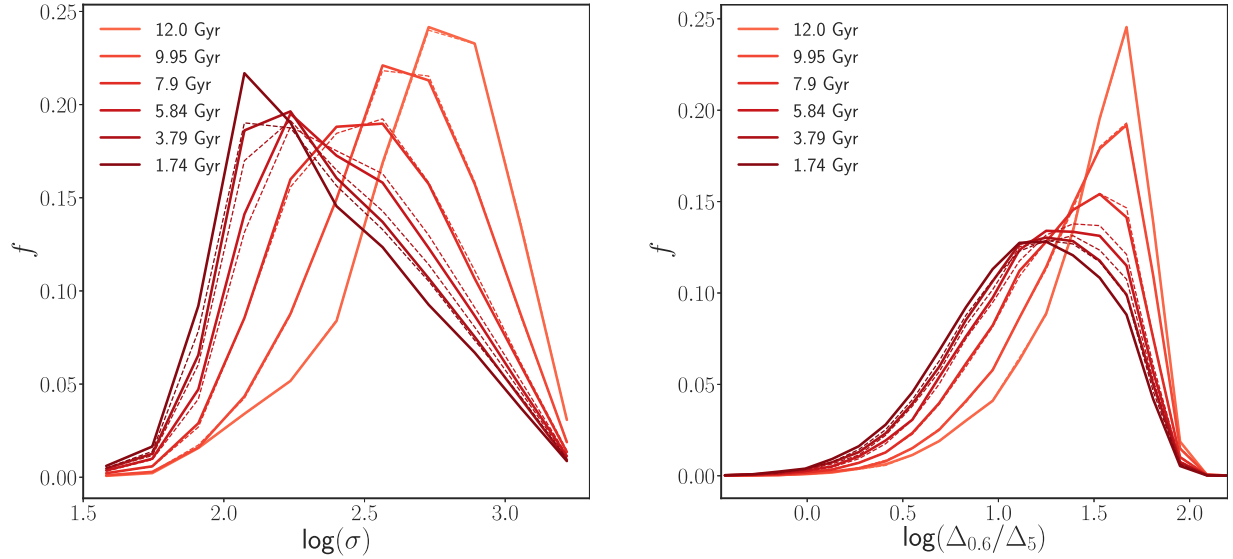
**Figure 5.** (Left) Distribution of logarithmic velocity dispersions, $\log \sigma$, for parent halos of BNS mergers, as a function of delay times. The dispersions are given in units of km/s. Velocity dispersions are a proxy for the parent halo mass, where mergers with long delay times tend to occur in higher mass halos. (Right) Distribution of the ratio of enclosed densities within 0.5 Mpc $h^{-1}$ and 5 Mpc $h^{-1}$ around hosts of BNS mergers, as a function of delay times, $\Delta_r = \Delta_{0.6}/\Delta_5$. The solid lines correspond to $\alpha = -1$, while the dashed line corresponds to $\alpha = -1.5$, where $\alpha$ denotes the slope of the merger time distribution function.
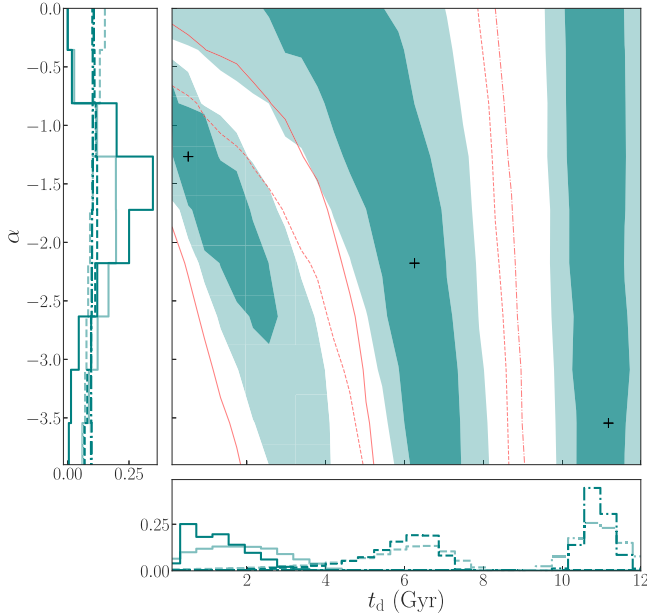


**Figure 6.** Posterior probability distribution of the slope and minimum delay of the time-delay distribution, as inferred for samples of 100 (dark green) and 30 (light green) host galaxies, drawn from three different delay time models (crosses denote the truth), using the complete set of observables, [$M_*$, sSFR, $\sigma_h$, $\Delta_r$]. The 1D, marginalized probabilities of the delay time and slope are shown in the bottom and left panels, respectively. The red contours correspond to the constraints obtained from 30 host galaxies, using only their stellar mass. The solid, dashed, and dotted–dashed lines correspond to injected delay times (crosses) in order of increasing magnitude. We take flat priors on $\alpha$ and $t_d$, so that the posterior is proportional to the likelihood. The contours enclose the area under 90% of the peak probability.
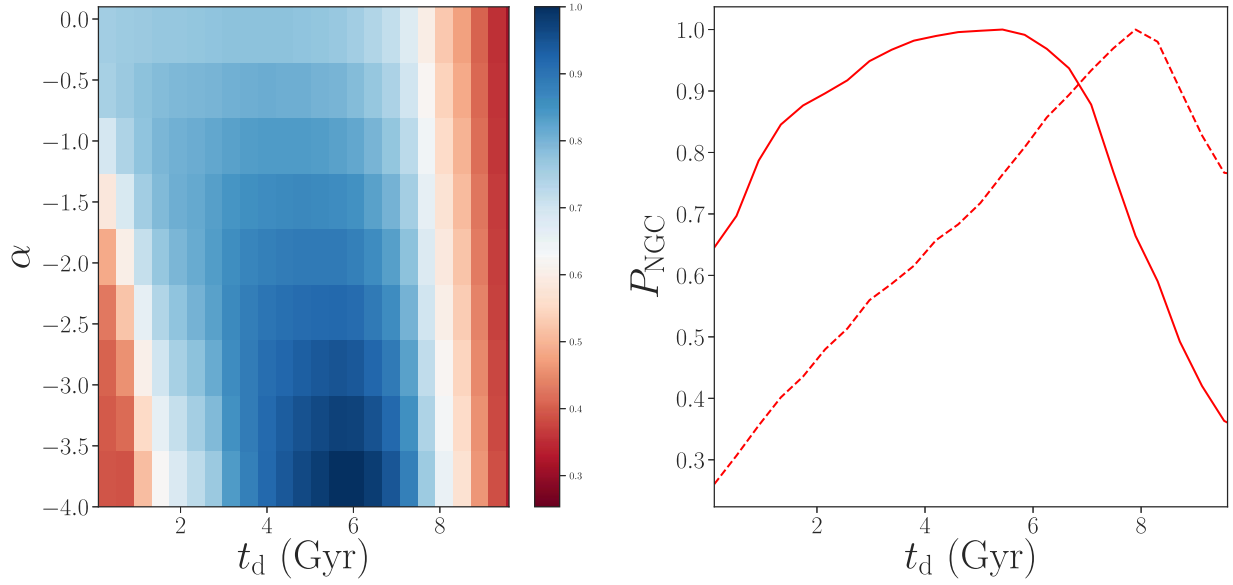
Figure 7 shows the probability of different time-delay distributions, given the star formation rate and stellar mass of NGC 4993. We find that NGC 4993 prefers a time-delay distribution with a minimum delay time longer than $\sim 1$Gyr, and a relatively steep slope. The right-hand panel of Figure 7 shows the probability of different delay times when we marginalize over $\alpha$ with a flat prior in the range

$-4 < \alpha < 0$. The preference for intermediate delay times is a consequence of the fact that NGC 4993 has a somewhat low average sSFR, given its stellar mass.

The value of SFR quoted by Artale et al. (2020), which corresponds to the solid curve in the right panel of figure 7, is the average star formation rate over a Gyr. We note that NGC 4993 prefers an even longer delay time when we use the current star formation rate of $0.01 M_\odot$ yr$^{-1}$ given by Belczynski et al. (2018) and Im et al. (2017). The dashed line in Figure 7 shows the probability of a delay time, adopting the value given in Belczynski et al. (2018). It appears that in this case, NGC 4993 prefers a delay time closer to $\sim 8$ Gyr.

Another aspect of NGC 4993 explored in the literature is the fact that it is not an isolated field galaxy, but appears to be associated with a group of galaxies. Palmese et al. (2017) also found evidence for a dynamically driven formation for NGC 4993 based on the existence of stellar streams in its photometry. As the number of GW events increase, it is of interest to ask how often the hosts of GW events tend to be satellite systems, as opposed to isolated galaxies. We know from simulations that the fraction of satellite galaxies at a given stellar mass does not exceed 30%; comparing the satellite fraction of BNS host galaxies with the satellite fraction of all galaxies may be informative in relation to the astrophysics of BNS systems.

Table 2 in Howlett & Davis (2020) provides a summary of the properties of the galactic group hosting NGC 4993 as a satellite. We note that it appears that there is significant inconsistency in the properties of the host group among the different works cited in the table. The measured velocity dispersion and richness of the group, for example, exhibit a large degree of scatter. We also note that the most recent estimated virial radius of the group is 0.36 Mpc $h^{-1}$ (Kourkchi & Tully 2017), which corresponds to a parent dark matter halo virial mass of $\sim 10^{13} M_\odot$ $h^{-1}$); the velocity dispersion reported in previous studies is too small for such an object. In Figure 8 we plot the projected phase space distribution of the member galaxies of the group hosting NGC 4993, based on Kourkchi & Tully (2017).

**Figure 7.** (Left) Probability of NGC 4993 hosting the merger event GW17087 for different merger time distributions, with slope $\alpha$, and delay times $t_d$, where SFR $= 0.5 M_\odot \, \mathrm{yr}^{-1}$ (averaged over a Gyr). (Right) The probability of a given delay time, marginalizing over all values of the slope. The dashed line corresponds to the probability where SFR $= 0.01 M_\odot \, \mathrm{yr}^{-1}$, and the solid line corresponds to SFR $= 0.5 M_\odot \, \mathrm{yr}^{-1}$. The probability distribution is sensitive to the value of star formation rate. For the higher value of SFR (solid), NGC 4993 shows a slight preference for an intermediate delay time; the lower value shows a preference for a delay time $\sim 8$ Gyr.
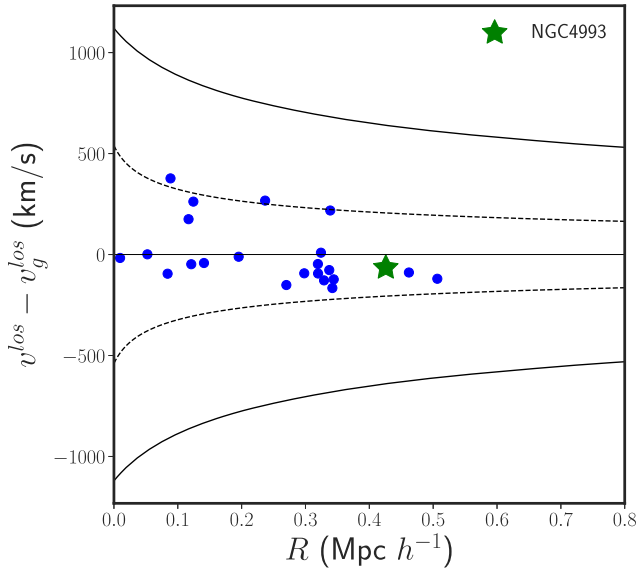


**Figure 8.** Projected phase space of galaxies in the group associated with NGC 4993. The black lines correspond to the escape velocity curves around a host halo of mass $10^{13} M_\odot h^{-1}$ (solid) and $10^{12} M_\odot \, h^{-1}$ (dashed).

The escape velocity envelope (denoted by the black solid line) of a $10^{12} M_\odot$ galaxy is more representative of the population claimed to be associated with the group; such a halo has a virial radius of $\sim 0.2 \, \mathrm{Mpc} \, h^{-1}$ which would place NGC 4993 on the outskirts of this group. Given the evidence for a dynamically driven formation of this galaxy, it is possible that NGC 4993 is a galaxy within the splashback radius of the group. However, its high stellar mass also makes it less likely to be at a large halo-centric distance from a group whose halo mass is as low as $10^{13} M_\odot$, as dynamical friction will draw it toward the center of the halo, unless it is on the first infall.

In summary, the star formation rate and stellar mass of NGC 4993 already provide important insights into the properties of BNSs. While the properties of the parent halo contribute additional information regarding BNS formation, it appears that further investigation is required to ascertain the parent halo mass of NGC 4993. As the sample of GW events increases, it will be useful to cross-correlate them with existing group and cluster catalogs, or to follow up their host galaxies with spectroscopy, so as to obtain the dynamical mass of the parent halo from neighboring galaxies, in order to better understand the binary–host connection.

### 3.3. Survey Strategy

As shown in the previous sections, different BNS formation models affect the population of their host galaxies. The previous sections were concerned with using observations of host galaxies in order to uncover the underlying formation models. However, in this section, we discuss the inverse problem, focusing on how a known formation model can aid the observational follow-up effort and help identify the most likely host galaxies. In a three-detector network, the GW signal can typically localize a BNS source to a few tens of thousands of $\mathrm{Mpc}^3$ in the sky, leading to hundreds of potential host galaxies in the 90% credible volume (Chen & Holz 2017). Many optical telescopes searching for a counterpart within a large volume rely on a pointing strategy to target the most probable galaxies first (Singer et al. 2016; Ducoin et al. 2020; Arcavi et al. 2017; Antolini et al. 2017). Moreover, identifying the most probable galaxies in a given volume (and assigning their relative probabilities of hosting a BNS merger) is integral to the galaxy catalog-based approach to measuring the Hubble constant (Schutz 1986; Fishbach et al. 2019).

The left panel of Figure 9 shows, for different delay time distributions, the stellar mass threshold required to capture 90% of all BNS events in the local universe. As different delay time distributions trace the stellar content of the universe in different ways, we see that the stellar mass threshold increases with the delay time of the merger. For the shortest delay times, with a minimum time-delay $\leqslant 1$ Gyr, galaxy catalogs would need to go to a stellar mass depth of $M_* = 10^8 M_\odot \, h^{-1}$ to capture 90%
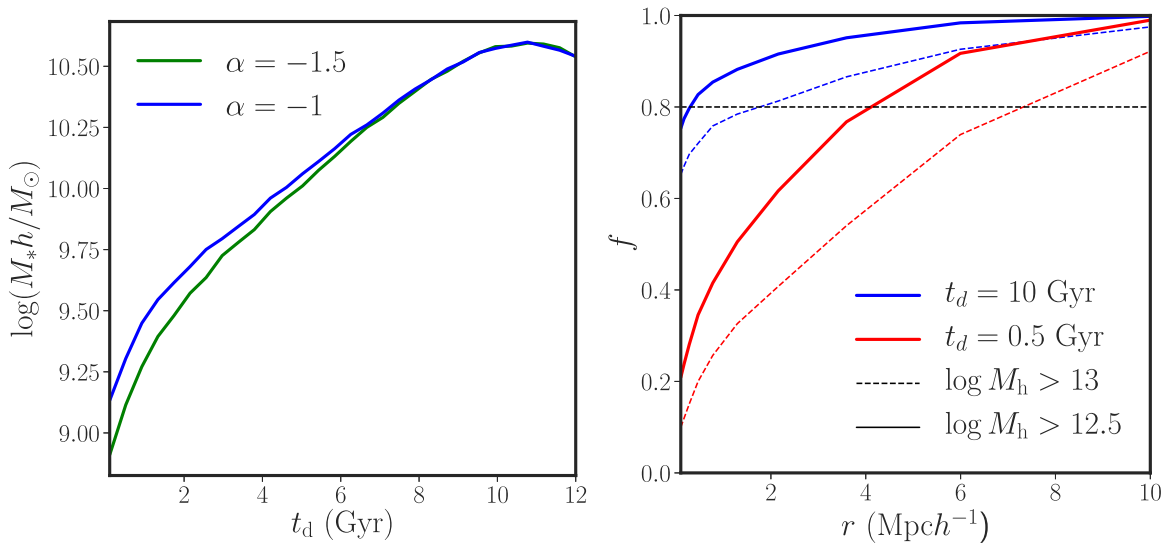
**Figure 9.** (Left) Stellar mass enclosing 90% of potential counterparts of BNS gravitational wave events, as a function of delay time. The different colors correspond to different slopes of merger time distributions, $\alpha$. (Right) The fraction of events enclosed within a radius $r$ of group mass halos above $M_{\rm h} > 10^{13}M_\odot h^{-1}$ (dotted lines) and $M_{\rm h} > 10^{12.5}M_\odot h^{-1}$ (solid lines), for two different time-delay models with minimum time-delay $t_{\rm d} = 10$ Gyr (blue) and $t_{\rm d} = 0.5$ Gyr (red). These curves assume a slope of the time-delay distribution of $\alpha = -1.5$. These clustering statistics are calculated using a 250 Mpc $h^{-1}$(per side) simulation box.

of BNS events. This corresponds to $\sim 0.01 M_*^{\rm MW}$. A galaxy survey such as the Dark Energy Spectroscopic Instrument (DESI) (Aghamousa et al. 2016), which is complete up to $r$-band magnitude $\sim 19.5$, would be able to observe a complete sample at the stellar mass threshold, out to $z = 0.05$.

While the depth of the survey is important for any follow-up strategy that searches through a galaxy catalog for a counterpart, another possible follow-up strategy may be to start with a cluster or group catalog, then to search the vicinity of the most massive halos. The success of such a strategy depends on the clustering of GW events.

Massive halos formed from the collapse of rare peaks in the early universe tend to cluster together (Kaiser 1984; Efstathiou et al. 1988; Bond et al. 1991; Mo & White 1996). Galaxies growing in the potential wells of halos also trace the clustering of their parent halos at all scales (Kaiser 1984). Moreover, as discussed above, the stellar mass of a galaxy and its total dark matter content are correlated. Therefore, if the BNS merger rate traces stellar mass, BNS events are more likely to be clustered within the vicinity of the most massive objects in the universe. Because the halo mass function falls off steeply at the high-mass end (Press & Schechter 1974), searching for BNS counterparts around group mass objects may significantly improve the efficiency of the search, without requiring a deep galaxy catalog.

However, the clustering of BNS host galaxies, as is the case for other galactic properties, is a function of the underlying delay time model. For different models, the BNS merger rate traces the stellar mass of a galaxy in different ways. Moreover, as discussed, the star formation history of a galaxy is environment-dependent (Balogh et al. 1997; Baldry et al. 2006). We find that for long delay times, BNS host galaxies are typically found within a smaller radius to a massive galaxy. The right panel of Figure 9 shows the fraction of BNS events captured within spheres of different radii around the most massive halos. The solid and dashed curves correspond to halos with a mass greater than $10^{13}M_\odot h^{-1}$ and $10^{12.5}M_\odot h^{-1}$,

respectively. Whereas for long delay times we can cover $\sim 80\%$ of potential host galaxies by targeting the region within a few Mpc around the $10^{13}M_\odot\, h^{-1}$ groups, for shorter time delays, a group catalog covering lower halo masses would be more optimal.

Figure 10 shows the distribution of GW events in the simulation box over a $50\,{\rm Mpc}\, h^{-1}$ slice. The left and right panels correspond to the distribution for a short and long delay time, respectively, bracketing our range of parameters. As we saw in Figure 9, GW events at $z = 0$ are more clustered when they have long delay times, as compared to short ones. This is related to the fact that for long delay times, GW events trace galaxies with high stellar mass, whose star formation peaked at earlier times, compared with low $M_*$ galaxies. The more massive galaxies tend to inhabit massive halos, which form out of the collapse of rarer peaks in the early universe, and tend to cluster together.

In this paper, we explore how the delay time distributions of BNS mergers moderate the observed properties of the host galaxies, and how their observed distributions can be used to understand the formation of binaries in the universe. We note however, that we have not considered the complete array of selection effects that may potentially arise in observations. For example, measuring stellar mass and star formation histories can be systematically more challenging for BNS mergers in faint galaxies, leading to a biased inference of the delay time distributions in favor of longer delay times. Another possibility is that BNS mergers in faint satellites of massive halos may be incorrectly associated with the more massive central galaxy of the host halo, and the offset between the host and the site of the kilonovae can be attributed to a displacement from velocity kicks (Lipunov et al. 1997; Fryer et al. 1998) occurring during mergers. We note that while targeted spectroscopic follow-up of energetic electromagnetic events may mitigate these effects to some extent, a systematic study of the interplay between theoretical models and observational inferences is an important direction for future investigation.
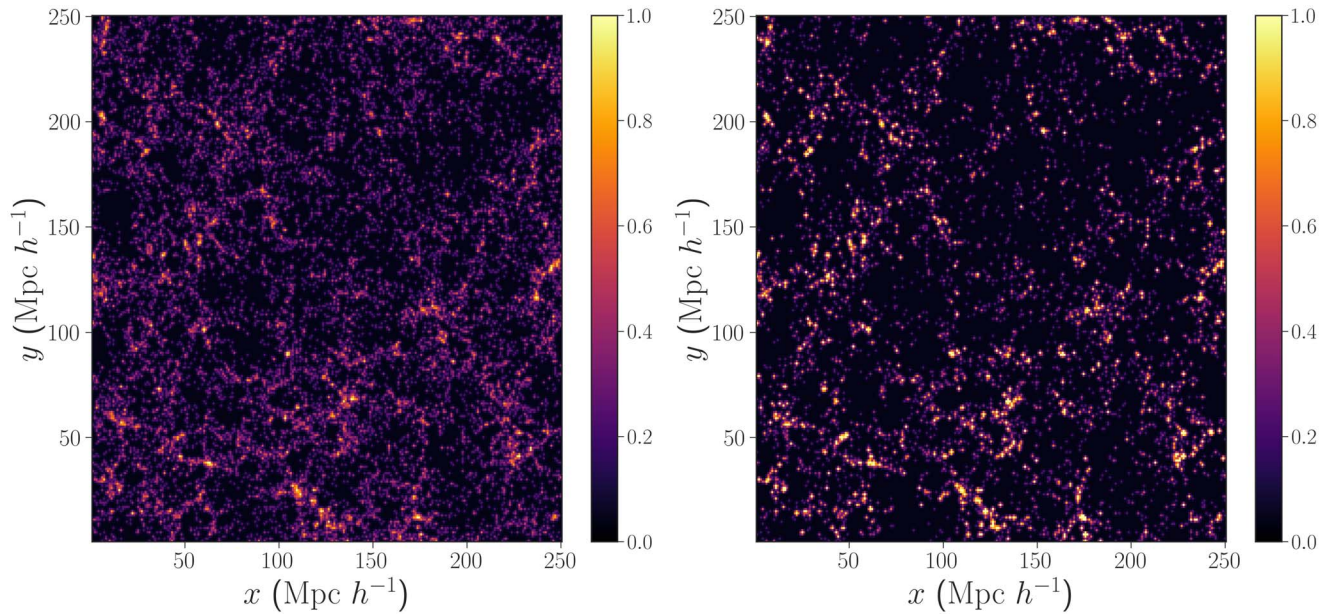
**Figure 10.** Distribution of GW events in space, taken from our simulations. The left panel corresponds to a delay time of 500 Myr, while the right panel corresponds to a delay of 10 Gyr. The color bar corresponds to the logarithmic density of events. The GW events are more clustered for long delay times (right) because most of these events occur in the high stellar mass objects that dominated star formation at a lookback time of 10 Gyr. High $M_*$ galaxies live in high-mass halos that tend to cluster more strongly. These plots assume a slope of $\alpha = -1.5$ for the time-delay distribution.

## 4. Summary and Conclusion

We have used the UniverseMachine galaxy evolution model to predict the formation and merger of BNSs over cosmological time. This allows us to relate astrophysical properties of the evolution of binaries detected by GW networks to the observable properties of their host galaxies.

We estimate the rate of mergers for each galaxy at $z = 0$ from merger time models parameterized by the slope of the time-delay distribution, $\alpha$, and the minimum delay time, $t_d$, in order to construct mock observations of GW events, and to study the properties of their hosts. The current generation of GW detectors, such as Advanced LIGO/Virgo and LIGO A+, are expected to detect tens to hundreds of BNS mergers and counterparts in the coming years. We show that the combination of events from current GW detectors with current and future galaxy surveys is a particularly promising avenue for research, allowing us to make significant inferences regarding the underlying astrophysical population of binaries. The main findings of our work are:

(i) With a sample of $\mathcal{O}(10)$ host galaxies to GW events, it is possible to distinguish formation models that predominantly trace stellar mass, star formation rate, or parent halo mass, both from each other and from a random selection of galaxies (see Figure 2). We note that with ∼30 host galaxies, it is possible to distinguish between halo mass weighting and stellar mass weighting, and thereby distinguish between the associated formation channels of binary systems in globular clusters, as opposed to galaxies.

(ii) Using the distribution of observable galaxy properties (i.e., stellar mass, star formation rate, halo velocity dispersion, and local density), we find that with an order of a few tens of events, we can distinguish short and long delay times at $\gtrsim 3\sigma$ (see Figure 6). For longer delay times, we encounter an inability to constrain the slope of

the merger time distributions. The addition of halo velocity dispersion information significantly improves the constraints, as compared to those obtained using only stellar mass and sSFR.

(iii) In the context of our single existing GW counterpart event, GW17087, we find that the properties of the host NGC 4993 favor a delay time of longer than a Gyr (consistent with previous work; see Levan et al. 2017; Pan et al. 2017; Belczynski et al. 2018). This can be attributed to the fact that NGC 4993 has a lower than expected star formation rate for its measured stellar mass. Using the current star-formation rate, we find that NGC 4993 shows a preference for a delay time close to 8 Gyr. Related to this is the inference that this host galaxy appears to be drawn from a stellar mass weighted, or a halo mass weighted sample. We also note that, whereas the literature has associated NGC 4993 with a bound group of galaxies, the measured velocity dispersion of the galaxies in the group suggest that the estimated virial radius of the group may not be representative of its true halo mass. The galaxies in the purported group appear to favor a $10^{12} M_\odot h^{-1}$ halo, with NGC 4993 at its outskirts.

(iv) In general, we find that the probability of a galaxy hosting a merger today is a function of the delay time model, where BNSs with short delay times preferentially exist in star-forming galaxies that inhabit halos similar to or lower in mass than the Milky Way, while mergers with longer delay times prefer more massive galaxies, which on average populate groups or clusters, and tend to be more clustered in space.

(v) Follow-up strategies to localize electromagnetic counterparts for gravitational wave events can be optimized by searching for transients around massive galaxy groups (see Figure 9). While the clustering of events is related to the underlying delay time distribution, we find that, even for short delay times, nearly 80% of all events can be captured by searching within a few Mpc of halos of mass

$M > 10^{12.5} M_\odot h^{-1}$. We also infer that if transients are not found around the most massive objects in the universe, this can be interpreted as favoring a model with short delay times. Although the study in this paper is limited to the low-redshift universe, consisting of a $250^3$ Mpc$^3$ $h^{-3}$ volume at $z = 0$, we note that the clustering of events is an important method of probing the underlying population of binary systems, and may also provide a potentially useful tool to optimize localization strategies for future surveys.

As galaxy surveys become more sophisticated, properties of galaxy hosts, such as halo velocity dispersions and 3D clustering, will potentially be measured with greater accuracy, using spectroscopic instruments such as DESI and WFIRST (Spergel et al. 2013; Aghamousa et al. 2016). Moreover, photometric surveys such as DES, HSC, and LSST (Abbott et al. 2005; Aihara et al. 2018; LSST Science Collaboration et al. 2009) could be used to measure clustering in projected space, which contains similar information about halo mass and environment. A systematic study of the properties of the host galaxies, including the properties of the parent halo and its spatial and temporal clustering as a function of delay time models, is a powerful tool for determining the underlying astrophysics of binary systems. In fact, we emphasize that folding in properties of the parent halo can provide important information to distinguish dynamical formation channels of binaries in dense stellar regions like globular clusters; the individual stars in these systems are not born as binaries and are not required to follow the power-law delay time models.

While GW17087 is the first gravitational wave associated with the confirmed merger of a BNS, related astrophysical phenomena, such as sGRBs, are also expected to result from mergers of BNSs; therefore a similar study of hosts of sGRBs could be used to constrain delay time models. In fact, GRB150101B, an sGRB similar to GW17087, and conjectured to be associated with a neutron star merger (Troja et al. 2018), also has a very low star-formation rate and a stellar mass similar to NGC 4993 (Xie et al. 2016). Furthermore, in scenarios where host galaxies can be identified, it will also be informative to study the distribution of other indicators of underlying formation mechanisms, such as offsets between the site of the merger and the host galaxy (Bloom et al. 1999; Perna & Belczynski 2002; Belczynski et al. 2002; Voss & Tauris 2003; Zevin et al. 2019), in relation to the properties of the hosts. For example, Kelley et al. (2010) studied the distribution of binary events in the local universe by modeling the natal velocity kicks that create such offsets in an $N$-body simulation. We also note that recent work has shown that a small fraction of BBH mergers (on order $\sim$1 per year) can be localized well enough to allow the identification of a unique host galaxy, despite not having the associated electromagnetic counterparts (Chen & Holz 2017). Therefore, a comprehensive follow-up of the properties of the host galaxies, including its halo mass, and its environment, along with its stellar mass and star formation history, may also provide a window into the formation models of binary black hole systems (Elbert et al. 2018). We note that Lamberts et al. (2016), Artale et al. (2020), and Artale et al. (2019) have made predictions regarding the host galaxy properties of BBH mergers, based on population synthesis models.

The advent of gravitational wave astronomy provides a new observational tool for probing the physics of binary systems;

the formation of galaxies, and their co-evolution with cosmological structure, on the other hand, has been studied extensively over the years, both theoretically and observationally through simulations and large-scale galaxy surveys. We show that, given the unique opportunity to identify a host galaxy for a gravitational wave event, the distribution of host properties, combined with knowledge of galaxy formation, can provide important information regarding the evolution of binaries through time. In the absence of an electromagnetic counterpart, an understanding of the binary–host connection may improve localization strategies for probable host galaxies. We emphasize that further studies of the connection between binaries and their hosts through the history of the universe, an exciting prospect, potentially leading to a better understanding of the cosmological and astrophysical information we can extract from gravitational wave sources.

### ORCID iDs

Susmita Adhikari ● https://orcid.org/0000-0002-0298-4432
Maya Fishbach ● https://orcid.org/0000-0002-1980-5293
Daniel E. Holz ● https://orcid.org/0000-0002-0175-5064
Risa H. Wechsler ● https://orcid.org/0000-0003-2229-011X

### References

Aasi, J., Abbott, B. P., Abbott, R., et al. 2015, CQGra, 32, 074001
Abbott, B. P., Abbott, R., Abbott, T. D., et al. 2017a, ApJL, 848, L13
Abbott, B. P., Abbott, R., Abbott, T. D., et al. 2017b, PhRvL, 119, 161101
Abbott, B. P., Abbott, R., Abbott, T. D., et al. 2017c, ApJL, 848, L12
Abbott, B. P., Abbott, R., Abbott, T. D., et al. 2017d, Natur, 551, 85
Abbott, B. P., Abbott, R., Abbott, T. D., et al. 2018, LRR, 21, 3
Abbott, T., Aldering, G., Annis, J., et al. 2005, arXiv:astro-ph/0510346
Acernese, F., Agathos, M., Agatsuma, K., et al. 2015, CQGra, 32, 024001
Aghamousa, A., Aguilar, J., Ahlen, S., et al. 2016, arXiv:1611.00036
Aghanim, N., Akrami, Y., Ashdown, M., et al. 2018, arXiv:1807.06209
Aihara, H., Arimoto, N., Armstrong, R., et al. 2018, PASJ, 70, S4
Alexander, K. D., Berger, E., Fong, W., et al. 2017, ApJL, 848, L21
Andrews, J. J., & Mandel, I. 2019, ApJL, 880, L8
Antolini, E., Caiazzo, I., Davé, R., & Heyl, J. S. 2017, MNRAS, 466, 2212
Arcavi, I., McCully, C., Hosseinzadeh, G., et al. 2017, ApJL, 848, L33
Artale, M. C., Mapelli, M., Bouffanais, Y., et al. 2020, MNRAS, 491, 3419
Artale, M. C., Mapelli, M., Giacobbo, N., et al. 2019, MNRAS, 487, 1675
Baldry, I. K., Balogh, M. L., Bower, R. G., et al. 2006, MNRAS, 373, 469
Balogh, M., Morris, S. L., Yee, H. K. C., Carlberg, R. G., & Ellingson, E. 1997, ApJL, 488, L75
Bardeen, J. M., Bond, J., Kaiser, N., & Szalay, A. 1986, ApJ, 304, 15
Behroozi, P., Wechsler, R., Hearin, A., & Conroy, C. 2019, MNRAS, 488, 3143

Behroozi, P. S., Wechsler, R. H., & Conroy, C. 2013a, ApJ, 770, 57
Behroozi, P. S., Wechsler, R. H., & Wu, H.-Y. 2013b, ApJ, 762, 109
Belczynski, K., Bulik, T., & Kalogera, V. 2002, ApJL, 571, L147
Belczynski, K., Bulik, T., Olejak, A., et al. 2018, arXiv:1812.10065
Berger, E., Fox, D. B., Price, P. A., et al. 2007, ApJ, 664, 1000
Blanchard, P. K., Berger, E., Fong, W., et al. 2017, ApJL, 848, L22
Bloom, J. S., Perley, D. A., Chen, H. W., et al. 2007, ApJ, 654, 878
Bloom, J. S., Prochaska, J. X., Pooley, D., et al. 2006, ApJ, 638, 354
Bloom, J. S., Sigurdsson, S., & Pols, O. R. 1999, MNRAS, 305, 763
Bond, J., Cole, S., Efstathiou, G., & Kaiser, N. 1991, ApJ, 379, 440
Brinchmann, J., Charlot, S., White, S. D. M., et al. 2004, MNRAS, 351, 1151
Brout, D., Scolnic, D., Kessler, R., et al. 2019, ApJ, 874, 150
Bullock, J. S., Kravtsov, A. V., & Weinberg, D. H. 2000, ApJ, 539, 517
Chen, H.-Y., Fishbach, M., & Holz, D. E. 2018, Natur, 562, 545
Chen, H.-Y., & Holz, D. E. 2017, ApJ, 840, 88
Conroy, C., & Wechsler, R. H. 2009, ApJ, 696, 620
Coulter, D. A., Foley, R. J., Kilpatrick, C. D., et al. 2017, Sci, 358, 1556
Croton, D. J., Gao, L., & White, S. D. M. 2007, MNRAS, 374, 1303
Dalal, N., Holz, D. E., Hughes, S. A., & Jain, B. 2006, PhRvD, 74, 063006
Dalal, N., White, M., Bond, J., & Shirokov, A. 2008, ApJ, 687, 12
Dominik, M., Belczynski, K., Fryer, C., et al. 2012, ApJ, 759, 52
Dressler, A. 1980, ApJ, 236, 351
Dressler, A., & Gunn, J. E. 1983, ApJ, 270, 7
Ducoin, J. G., Corre, D., Leroy, N., & Le Floch, E. 2020, MNRAS, 492, 4768
Efstathiou, G., Frenk, C., White, S. D., & Davis, M. 1988, MNRAS, 235, 715
Elbert, O. D., Bullock, J. S., & Kaplinghat, M. 2018, MNRAS, 473, 1186
Fishbach, M., Gray, R., Magaña Hernandez, I., et al. 2019, ApJL, 871, L13
Fishbach, M., Holz, D. E., & Farr, W. M. 2018, ApJL, 863, L41
Fong, W., & Berger, E. 2013, ApJ, 776, 18
Fong, W., Berger, E., Blanchard, P. K., et al. 2017, ApJL, 848, L23
Fryer, C., Burrows, A., & Benz, W. 1998, ApJ, 496, 333
Gao, L., & White, S. D. M. 2007, MNRAS, 377, L5
Grindlay, J., Portegies Zwart, S., & McMillan, S. 2006, Nature Phys, 2, 116
Guzman, R., Gallego, J., Koo, D. C., et al. 1997, ApJ, 489, 559
Harris, W. E., Harris, G. L. H., & Alessi, M. 2013, ApJ, 772, 82
Holz, D. E., & Hughes, S. A. 2005, ApJ, 629, 15
Hopkins, P. F., Quataert, E., & Murray, N. 2012, MNRAS, 421, 3522
Howlett, C., & Davis, T. M. 2020, MNRAS, 492, 3803
Hudson, M. J., Harris, G. L., & Harris, W. E. 2014, ApJL, 787, L5
Im, M., Yoon, Y., Lee, S.-K. J., et al. 2017, ApJL, 849, L16
Kaiser, N. 1984, ApJL, 284, L9
Kelley, L. Z., Ramirez-Ruiz, E., Zemp, M., Diemand, J., & Mandel, I. 2010, ApJL, 725, L91
Klypin, A. A., Trujillo-Gomez, S., & Primack, J. 2011, ApJ, 740, 102
Kobulnicky, H. A., Kiminki, D. C., Lundquist, M. J., et al. 2014, ApJS, 213, 34

Kourkchi, E., & Tully, R. B. 2017, ApJ, 843, 16
Kravtsov, A., Vikhlinin, A., & Meshscheryakov, A. 2018, AstL, 44, 8
Kravtsov, A. V., Berlind, A. A., Wechsler, R. H., et al. 2004, ApJ, 609, 35
Lamberts, A., Garrison-Kimmel, S., Clausen, D. R., & Hopkins, P. F. 2016, MNRAS, 463, L31
Leibler, C. N., & Berger, E. 2010, ApJ, 725, 1202
Levan, A. J., Lyman, J. D., Tanvir, N. R., et al. 2017, ApJL, 848, L28
Lipunov, V. M., Postnov, K. A., & Prokhorov, M. E. 1997, MNRAS, 288, 245
LSST Science Collaboration, Abell, P. A., Allison, J., et al. 2009, arXiv:0912.0201
Margutti, R., Berger, E., Fong, W., et al. 2017, ApJL, 848, L20
Mo, H., & White, S. D. 1996, MNRAS, 282, 347
Oemler, A. J. 1974, ApJ, 194, 1
Palmese, A., Hartley, W., Tarsitano, F., et al. 2017, ApJL, 849, L34
Palmese, A., Graur, O., Annis, J. T., et al. 2019, arXiv:1903.04730
Pan, Y. C., Kilpatrick, C. D., Simon, J. D., et al. 2017, ApJL, 848, L30
Perna, R., & Belczynski, K. 2002, ApJ, 570, 252
Peters, P. C. 1964, PhRv, 136, 1224
Phinney, E. S. 1991, ApJL, 380, L17
Press, W. H., & Schechter, P. 1974, ApJ, 187, 425
Prochaska, J. X., Bloom, J. S., Chen, H.-W., et al. 2006, ApJ, 642, 989
Safarzadeh, M., & Berger, E. 2019, ApJL, 878, L12
Safarzadeh, M., Berger, E., Ng, K. K. Y., et al. 2019, ApJL, 878, L13
Sana, H., de Mink, S. E., de Koter, A., et al. 2012, Sci, 337, 444
Schutz, B. F. 1986, Natur, 323, 310
Silk, J., & Rees, M. J. 1998, A&A, 331, L1
Singer, L. P., Chen, H.-Y., Holz, D. E., et al. 2016, ApJL, 829, L15
Soares-Santos, M., Holz, D. E., Annis, J., et al. 2017, ApJL, 848, L16
Spergel, D., Gehrels, N., Breckinridge, J., et al. 2013, arXiv:1305.5422
Tauris, T. M., Kramer, M., Freire, P. C. C., et al. 2017, ApJ, 846, 170
Toffano, M., Mapelli, M., Giacobbo, N., Artale, M. C., & Ghirlanda, G. 2019, MNRAS, 489, 4622
Troja, E., Ryan, G., Piro, L., et al. 2018, NatCo, 9, 4089
Vale, A., & Ostriker, J. P. 2004, MNRAS, 353, 189
Vigna-Gómez, A., Neijssel, C. J., Stevenson, S., et al. 2018, MNRAS, 481, 4009
Vitale, S., Farr, W. M., Ng, K. K. Y., & Rodriguez, C. L. 2019, ApJL, 886, L1
Voss, R., & Tauris, T. M. 2003, MNRAS, 342, 1169
Wechsler, R. H., & Tinker, J. L. 2018, ARA&A, 56, 435
Wechsler, R. H., Zentner, A. R., Bullock, J. S., & Kravtsov, A. V. 2006, ApJ, 652, 71
Xie, C., Fang, T., Wang, J., Liu, T., & Jiang, X. 2016, ApJL, 824, L17
Ye, C. S., Fong, W.-F., Kremer, K., et al. 2020, ApJL, 888, L10
Zevin, M., Kelley, L. Z., Nugent, A., et al. 2019, arXiv:1910.03598